Heat Treat 2019: Proceedings of the
30th ASM Heat Treating Society Conference
October 15–17, 2019, Detroit, Michigan, USA

Copyright © 2019 ASM International®
All rights reserved.
www.asminternational.org

Quenching Process Improvement Through Modeling

Stefan Habean, Justin Sims, Zhichao Li, and B. Lynn Ferguson
DANTE Solutions, Inc., Cleveland, OH, USA
sales@dante-solutions.com

Abstract

Computer modeling offers an excellent method to investigate heat treatment processes, especially processes that have quality issues, that are open to use of different alloys, or that are under development.[1-4] A recent presentation from Karlsruhe Institute of Technology[5] was an excellent example of this, where three variations of a novel tube quenching process showed experimental evidence that two of the processes resulted in tubes with cracks on the bore while the third process produced crack-free parts. Interested in investigating this in more detail using computer modeling, a study was initiated to investigate additional process variations to better understand the effect of quenching conditions on stresses and microstructural evolution in the part. With a goal of producing martensite and residual compressive stress in the bore of a 4140 steel tube, a matrix of hardening processes was developed and executed. Models examined heat transfer and also microstructural evolution, i.e. phase transformation kinetics. Results showed that the timing and rate of martensite formation, and bainite kinetics had a significant effect on both the in-process stress state and the residual stress state.

Introduction

This paper shows the benefit of computer modeling by investigating a novel quenching process. Computer simulation was used to understand the metallurgical events that occur when steel is heat treated. Using experimental work conducted at Karlsruhe Institute of Technology by Fabian Mühl, Stefan Dietrich and Volcker Schülze [5] as a basis for this modeling effort, a matrix of models was run to investigate the effects of heat transfer and phase transformation behavior on residual stress and microstructure in a relatively thick walled tube. The steel in question was AISI 4140, and the novel quenching process aimed to produce a martensitic microstructure and residual compression in the bore of a tube having an inner diameter of 4 mm and an outer diameter of 29 mm. The experiments at Karlsruhe were conducted using a high pressure water quench on the bore of the tube to produce residual compression instead of a mechanical procedure such as autofrettage. For further information on the Karlsruhe work, see reference 1. Their publication included process details such as heat transfer coefficients, time-temperature data, and residual stress contours for their experimental conditions. This information provided boundary conditions for use in our models.

An axisymmetric model of the small tube was developed, with a 2 mm inner radius and a 14.5 mm outer radius. The model initial conditions included a starting uniform temperature of 850° C, a fully austenitic microstructure, and a stress-free state. Since the aim of the model was to investigate ID and OD differences and the microstructural evolution through the tube thickness, only a single layer of elements was needed. The axisymmetric model assumed that heat flow occurred only radially, and the top and bottom mesh surfaces remained planar. Reference 1 reported values of heat transfer between 14 and 65 kW/(m^2*K), depending on pressure and flow rate.[5] Using these as a guide, a matrix was developed for investigation, and the conditions are listed in Table 1. For the high pressure, high flow rate water quench, a single value for heat transfer was used. This assumed that these conditions prohibited film and nucleate boiling. Air cooling entailed heat transfer that changed with surface temperature. Besides heat transfer, the effect of phase transfer kinetics for martensite and bainite formation was examined.

Table I. Matrix of models that were run.

Model	Bore Heat Transfer kW/(m^2*K)	OD Heat Transfer kW/(m^2*K)
1	65	Air cool
2	Air cool	65
3	65	65
4	35	35
5	35	Air cool
6	Air Cool	35
Other Models		
11	Effect of Bainite Kinetics	
7a	10	Air Cool
7b	Model 7 with Modified Kinetics	
1c	Model 1 with Modified Kinetics	

The software used for these models was DANTE®. The material property data resident in DANTE's database for AISI 4140 steel was applied to the tube section. A representative CCT curve from these data is shown in Figure 1. For examination of phase transformation kinetics effects, the rate of martensite formation was varied, as was the kinetics of bainite formation. Figure 2 shows a CCT diagram produced using the modified kinetics. The main modification to the martensite kinetics was to slow down the rate of formation, keeping the martensite start temperature the same between the two cases. The difference for the modified bainite kinetics

was to increase the mobility and the temperature range of formation.

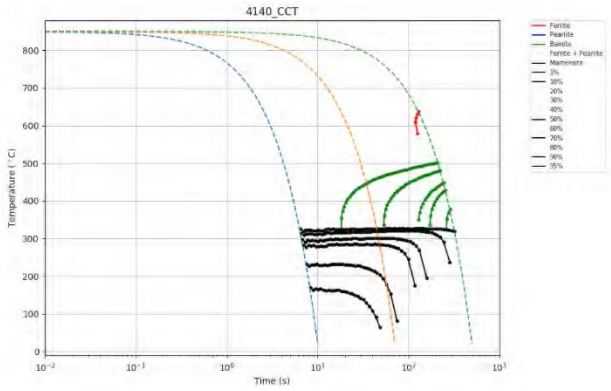

Figure 1. CCT curves generated for 4140 steel from the DANTE database.

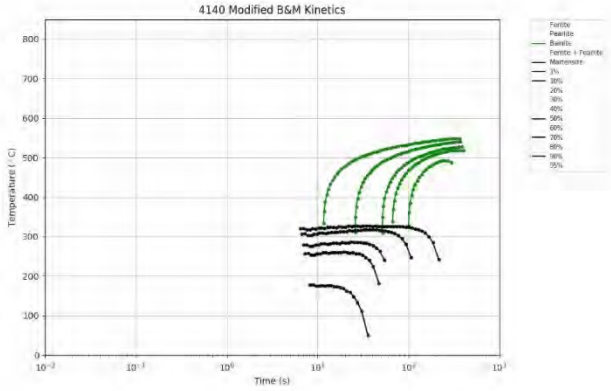

Figure 2. CCT curves for modified 4140 steel transformation kinetics.

The kinetics data reported in reference 1 has a similar martensite start temperature, but the bainite start time is about 8 seconds and the temperature range for bainite formation ranges above 500 C.

Modeling Results

Models 1 & 5: Primary Bore Cooling

Models 1 and 5 applied high heat transfer to the tube bore and air cooling to the OD, but the bore heat transfer in model 1 was nearly twice that of model 5. Both models used kinetics data from the DANTE database, shown graphically in Figure 1. Figure 3 shows the temperature vs. time curves for models 1 and 5 for the bore, mid-radius, and outer diameter locations. The line graphs show that the heat is mostly removed at the bore, as the bore is quenched rapidly in both models. Latent heat released during the rapid austenite to martensite transformation causes an interruption of cooling of about 30 seconds in the tube interior. The plateaus shown for the mid-radius (8 mm) and outer diameter locations are due to latent heat. Models run with the same kinetics data that have the latent heat set to zero showed no plateaus.

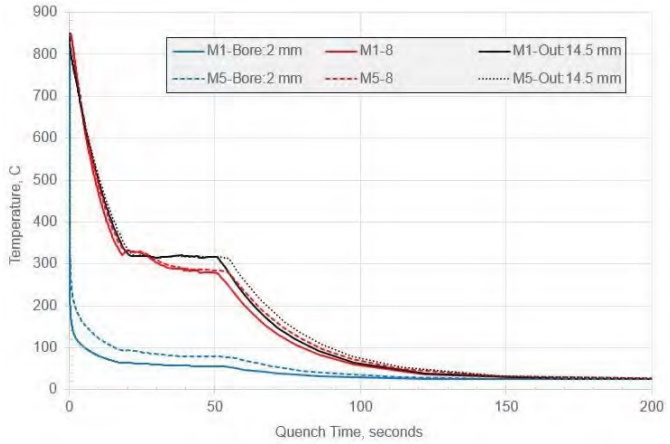

Figure 3. Temperature history graph for models 1 and 5 with high heat transfer on the bore and air cooling on the outer diameter.

The tangential or hoop stress in model 1 and the timing of martensite formation are shown in Figure 4. The time axis is plotted on a logarithmic scale for clarity since the bore cools so quickly. Martensite starts to form at the bore in about 0.1 seconds and is completed in less than 1 second. The thermal contraction of the bore is initially restricted by the hot body of the tube and hoop tension develops. As martensite forms at the bore, the material expansion reverses the direction of stress evolution and hoop compression is imposed at the bore. Several stress reversals at the bore are predicted as the progress of martensite formation takes place from the inner to the outer surface. Again, these stress reversals are due to thermal contraction with temperature loss and material expansion as martensite forms from austenite. The internal stress generated is sufficient to cause plastic strain in the austenite prior to transforming to martensite, see Figure 5. The level of plastic strain is highest in the bore and is predicted to decrease with radius, which mimics the timing of phase transformation from inside to outside in the tube. Remember, this is for conditions of high heat transfer in the bore.

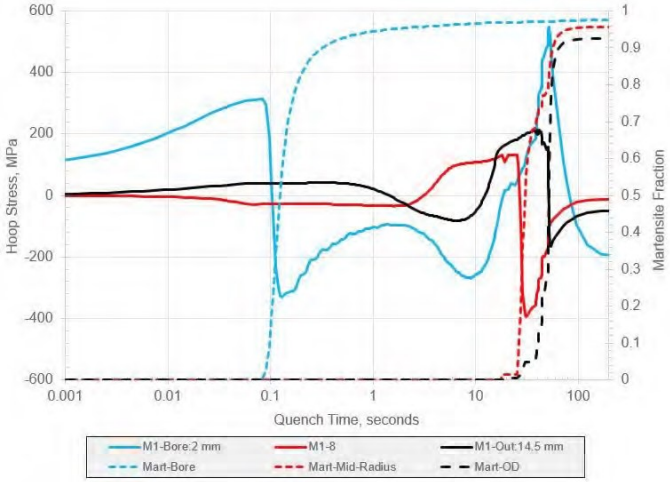

Figure 4. Hoop stress changes and martensite formation timing at the bore, mid-radius and outer diameter for model 1.

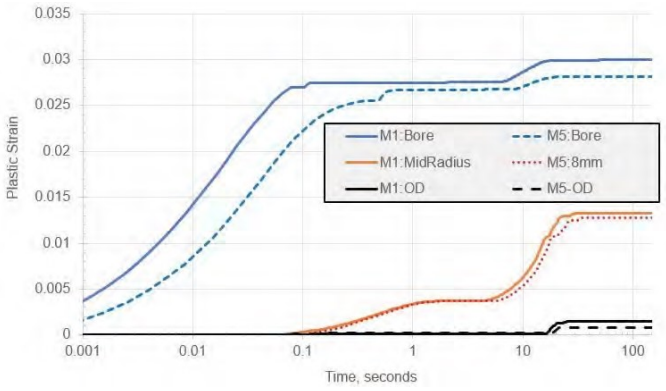

Figure 5. Plastic strain prediction for models 1 and 5 for the bore, mid-radius and outer diameter.

Models 2 & 6: Primary Outer Diameter Cooling

Models 2 and 6 investigate primary quenching at the outer diameter, with model 2 having a higher heat transfer coefficient than model 6, 65 vs. 35 kW/(m^2*K). The temperature history curves and martensite formation curves for model 2 are shown in Figure 6 for the bore, mid-radius and outer diameter; these models used rapid martensite formation kinetics. These curves look similar to the curves in Figure 2, except the faster cooling is now from the outside of the tube and martensite forms first at the OD and last at the bore. The plateau or interruption in cooling due to rapid latent heat release at both the mid-radius and bore are present. Because the outer diameter has a much larger surface area than the bore, the rate of heat extraction from the tube is higher for these models. The plateau at the mid-radius is not as pronounced as in Figure 3 and the overall cooling rate of the tube is faster than that of bore cooling.

Figure 7 shows hoop stress and martensite fraction vs. quench time for model 2. With martensite formation beginning at the outer diameter, the OD hoop stress is initially tensile as the surface tries to contract. As martensite forms, the stress becomes compressive, but thermal contraction and more significantly martensite formation beneath the outer surface causes tensile stress at the outer diameter. Again, there are several stress reversals predicted, and these are due to thermal contraction of the tube as it cools incrementally from the

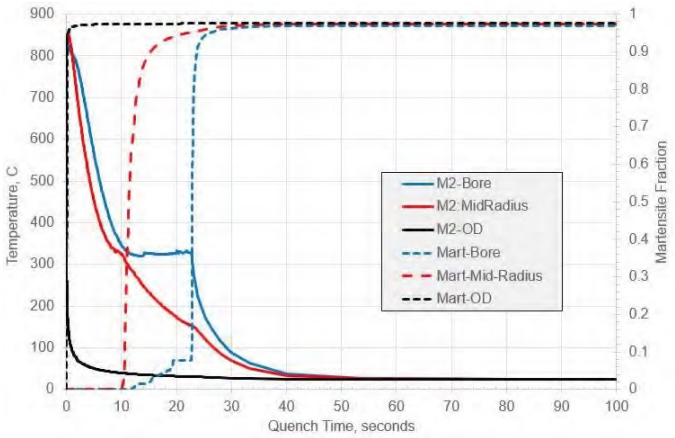

Figure 6. Temperature histories and martensite formation for the bore, mid-radius and outer diameter predicted for model 2.

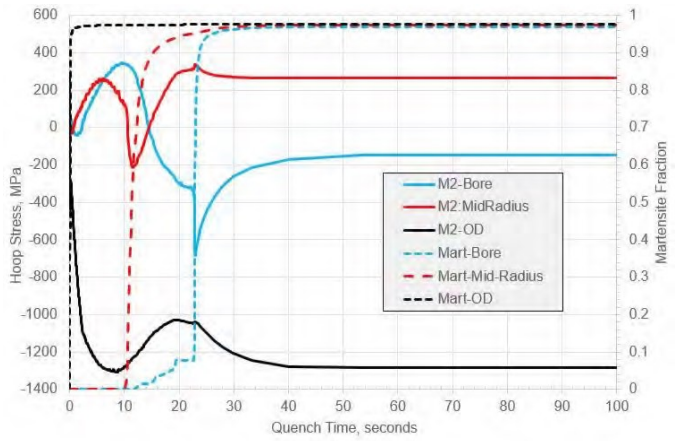

Figure 7. Hoop or tangential stress evolution and martensite formation predictions for model 2.

outside and to the dimensional expansion when martensite forms. Because martensite forms last at the bore, the magnitude of hoop compression is large, almost 1300 MPa. Figure 8 shows that the final radial contraction at the bore maintains the high bore surface compression.

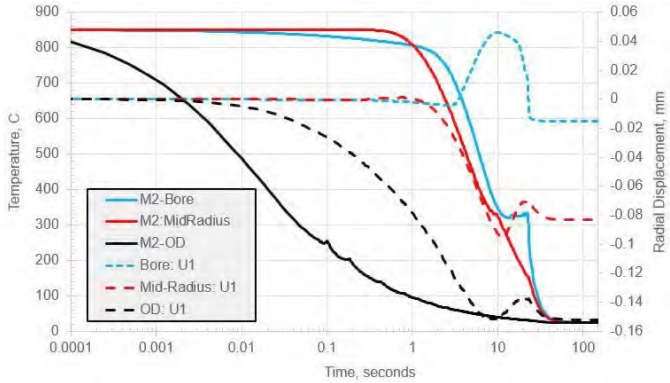

Figure 8. Temperature and radial displacement histories for model 2. Note: starting dimension is at 850 C.

While model 6 results are not shown in this grouping of figures, the results are similar to model 2. Because the heat transfer is half that of model 2, the cooling rate in model 6 is

less than that of model 2, but the final hoop stress on the OD is predicted to be -1,120 MPa and -148 MPa at the bore.

Models 3 & 4: Primary Cooling at Both OD and Bore

Models 3 and 4 both assumed high heat transfer during quenching on the bore and on the outer diameter. As with the other models presented thus far, martensite formation had a high rate. Figure 9 shows the predicted temperatures at the bore, mid-radius and the outer diameter. The mid-radius prediction shows a short plateau due to latent heat generation during martensite formation. The outer surface area is greater than the bore surface area and for the same heat transfer coefficient, the outer surface is predicted to cool faster than the bore surface. Of course, model 3 with a higher convective heat transfer coefficient cools faster than model 4. However, the steel thermal diffusivity limits the cooling of the tube interior so the cooling at mid-radius is nearly identical for these models.

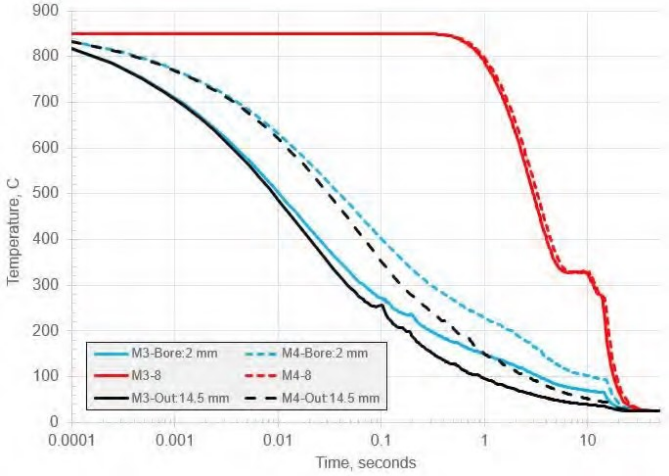

Figure 9. Temperature histories for models 3 and 4 showing the bore, mid-radius and outer diameter predictions.

The timing of martensite formation at the bore, mid-radius and outer diameter is shown for models 3 and 4 in Figure 10. The surfaces transform from austenite to martensite first, from about 0.06 seconds to 0.12 seconds for model 3 and 0.2 seconds to 12 seconds for model 4. The outer surface transforms before the bore surface in both cases. The mid-radius location transforms over about 10 to 20 seconds of quenching, and the transformations occur at nearly the same time range for both models.

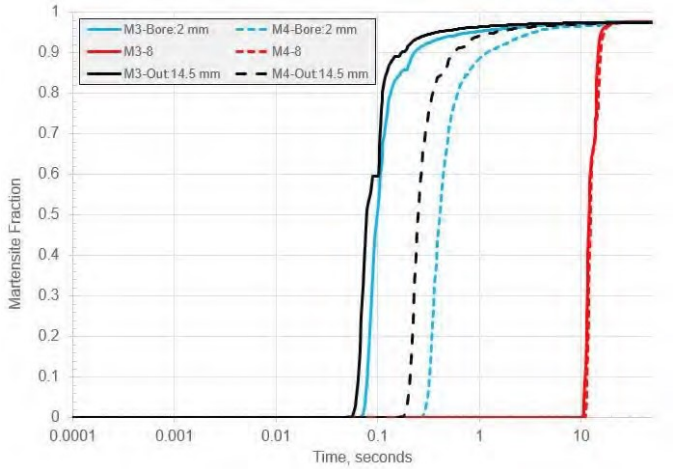

Figure 10. Martensite formation at the bore, mid-radius and outer diameter form models 3 and 4.

Hoop stress predictions for these same locations are shown in Figure 11. As with other models, there are several stress reversals that are associated with thermal stress during quenching and with phase transformations that occur. In these models, both the outer and bore surfaces have significant residual compression. The outer surface is predicted to have greater compression than the bore surface. Interestingly, mid-radius also is predicted to be under residual compression, but at a much lower magnitude. Figure 12 shows a graph of final hoop stress across the tube interior. The compression on the outer wall is shallow, giving way to circumferential tension at just over 1 mm depth beneath the outer surface. This tensile zone extends inward almost to mid-radius. From mid-radius inward, the compression magnitude is fairly low. The net effect is a balanced internal stress state.

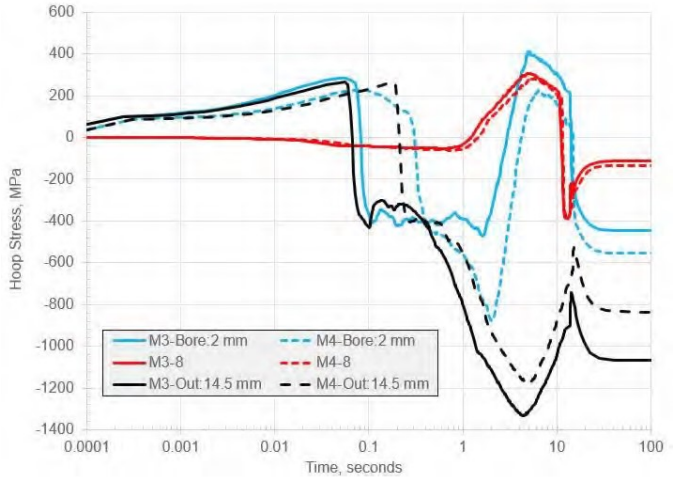

Figure 11. Hoop or tangential stress prediction for models 3 and 4 that have high heat transfer at both bore and outer diameter.

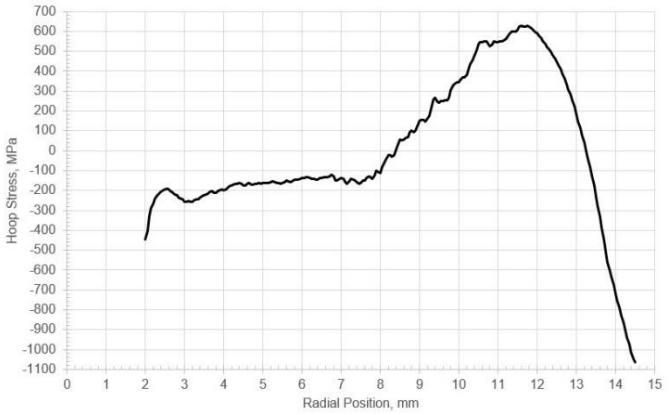

Figure 12. Final residual hoop stress predicted, showing stress from bore to outer diameter.

Figure 13 reports phase fractions of austenite, martensite, and also plastic strain at the bore, mid-radius and outer diameter of the tube during a model 3 quench (high heat transfer on bore and OD surfaces). The plastic strain at the bore and the outer dimeter are on the order of 2.5%, while the mid-radius has a plastic strain of 1.4%. The bulk of the plastic strain occurs in austenite due to thermal stress before martensite formation begins. But additional plastic strain does occur in austenite as the martensite forms in neighboring or adjacent regions. This additional strain is due to lattice expansion as the face centered cubic (FCC) austenite transforms to the less dense body centered tetragonal (BCT) martensite. The much stronger martensite endures the internal stress that is generated while the austenite plastically deforms.

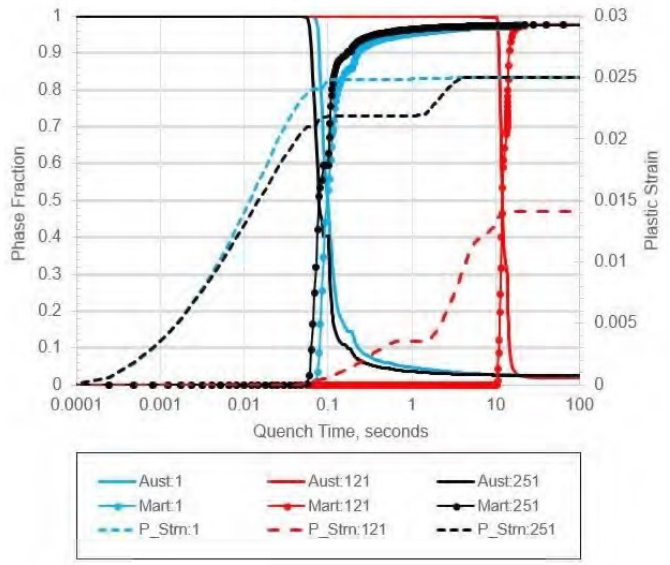

Figure 13. Model 3 predictions for austenite fraction, martensite fraction, and plastic strain at the bore, mid-radius and outer diameter.

Model 11: Effect of Bainite Kinetics

Model 11 explored the effect of bainite formation kinetics on residual stress state. The heat transfer conditions of model 1 were assumed, with the bore cooling very fast and the outer diameter cooling slowly. The change in bainite kinetics was to enhance the mobility term so that bainite would form more readily. Figure 14 shows the modified CCT that was produced for a minor adjustment in mobility. While the nose 1% curves are nearly the same, the 50% and 90% curves show the effect of increased mobility. Also, the curves for the modified kinetics lie in a higher temperature range. The result is that bainite should be easier to form, i.e. somewhat reduced hardenability for the modified kinetics.

The reduced hardenability for the modified bainite kinetics is evidenced in Figure 15 by the bainite amounts of 40% and higher present from mid-radius to the outer diameter. The comparative case for standard kinetics is shown in Figure 16, where bainite amounts are less than 10% at all radial positions. Figure 15 shows that the residual hoop stress at 1 mm depth from the bore is compressive, but outside of mid-radius the hoop stress is tensile. Figure 17 shows a direct comparison of the predicted residual hoop stress for the two kinetics cases. The modified kinetics produced deeper compressive stress than the standard kinetics, and the stress remained compressive until about mid-radius. The standard kinetics resulted in hoop tension after 1 mm of depth from the bore. Both kinetics cases resulted in hoop tension at the outer diameter, but the magnitudes are low, about 60 MPa and lower.

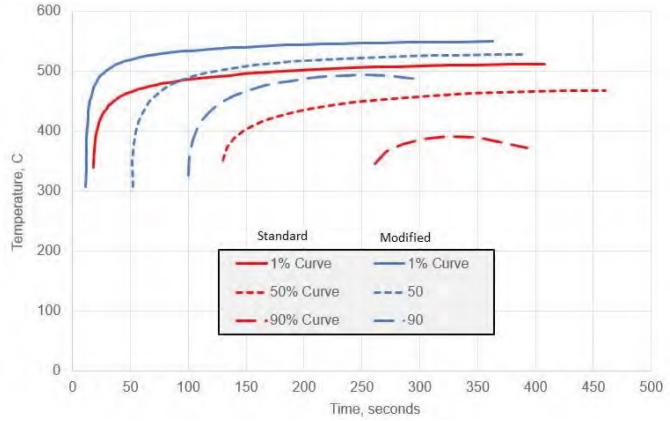

Figure 14. Bainite formation kinetics for 4140 steel from DANTE database and modified kinetics.

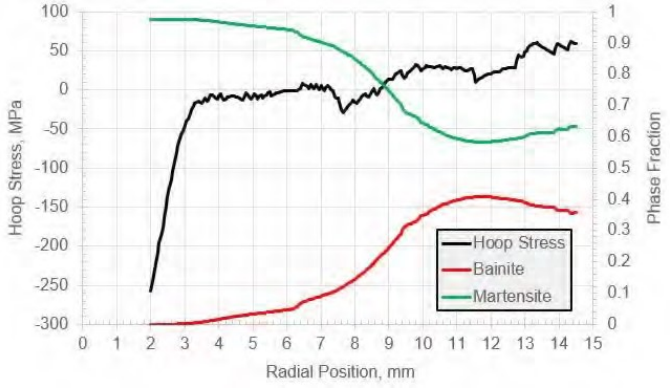

Figure 15. Predicted hoop stress, martensite fraction and bainite fraction for tube with modified kinetics quenched with high heat transfer at bore and air cooling on OD.

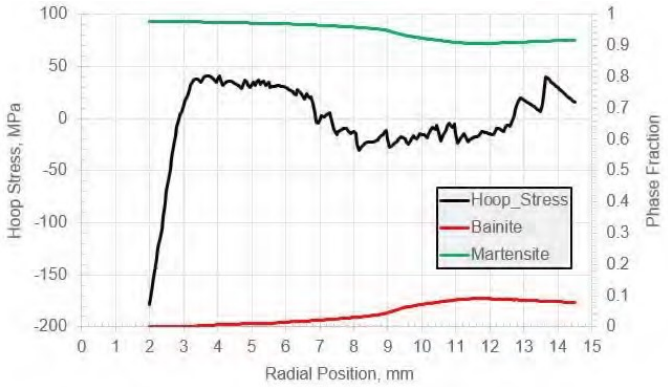

Figure 16. Predicted hoop stress, martensite fraction and bainite fraction for tube with standard kinetics quenched with high heat transfer at bore and air cooling on OD.

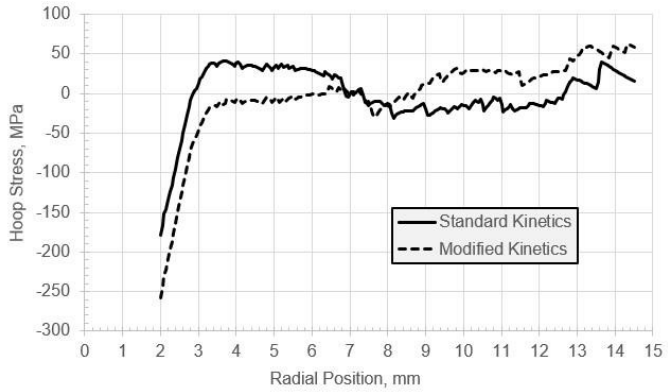

Figure 17. Comparison of predicted residual stress across tube for standard and modified bainite kinetics.

Models 7a & 7b: Effect of Martensite Kinetics

Models to this point have used martensite kinetics that have a high rate of formation, meaning that a significant amount of martensite quickly forms as temperature falls below the martensite start temperature. As Figures 3, 6, 8 and 9 have shown, this results in rapid release of latent heat that requires some time for conduction to catch-up with heat release – hence the time-temperature plateaus that are predicted. Figure 2 shows martensite formation with a slower rate of formation so that latent heat release is spread over a longer time period as cooling occurs.

Figure 18 shows temperature vs. time plots for models 7a and 7b. The heat transfer at the bore is 10 kW/(m^2*K) in both models with air cooling at the outer diameter. However, model 7a uses kinetics shown in Figure 1 and model 7b uses kinetics shown in Figure 2. The lower rate of martensite formation in model 7b allows latent heat to be conducted away faster than it is generated, and no plateau is present. The effective cooling rate is higher in model 7b than in 7a. Figure 19 shows the martensite formation for these models, and it is clear that martensite forms earlier in model 7b because the interior temperature drops below Ms earlier. Model 7a actually forms a higher amount of interior martensite because the bainite

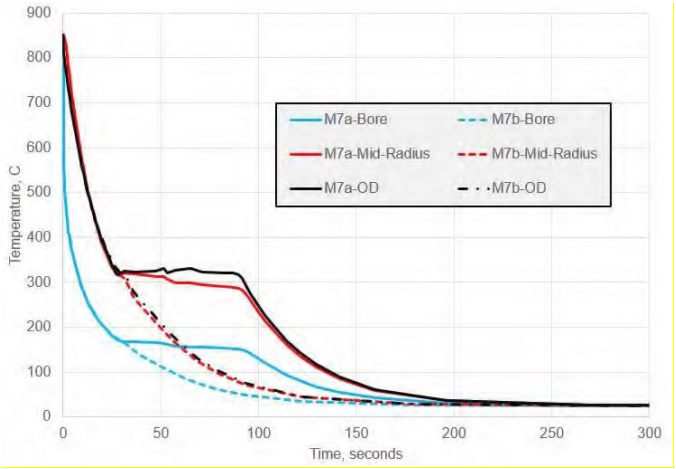

Figure 18. Temperature histories for bore, mid-radius and outer diameter for models 7a and 7b showing the difference due to rate of martensite formation.

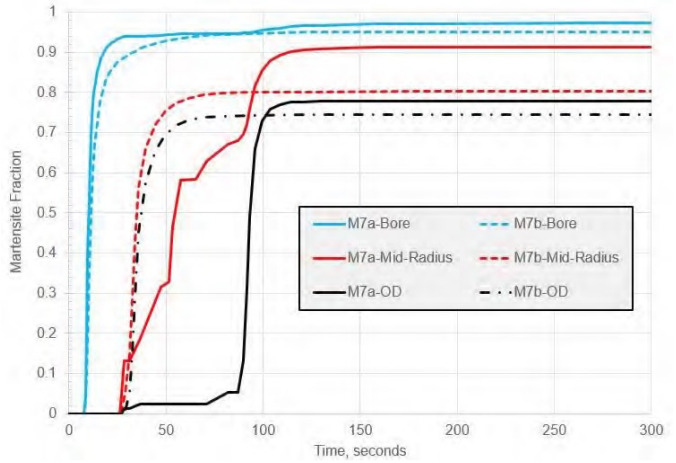

Figure 19. Martensite formation at the bore, mid-radius and outer diameter for models 7a and 7b.

kinetics are faster in model 7b and some bainite forms in the interior.

Figure 20 compares the evolution of hoop stress at the bore, mid-radius and outer diameter for models 7a and 7b. For this heat transfer magnitude at the bore and the material kinetics differences, the timing of the stress reversals is different between the models, but the final outcome is that residual stress is predicted to be low in the tube for both models 7a and 7b. For the much higher heat transfer at the bore in model 1, the predicted hoop stress was about -200 MPa at the bore.

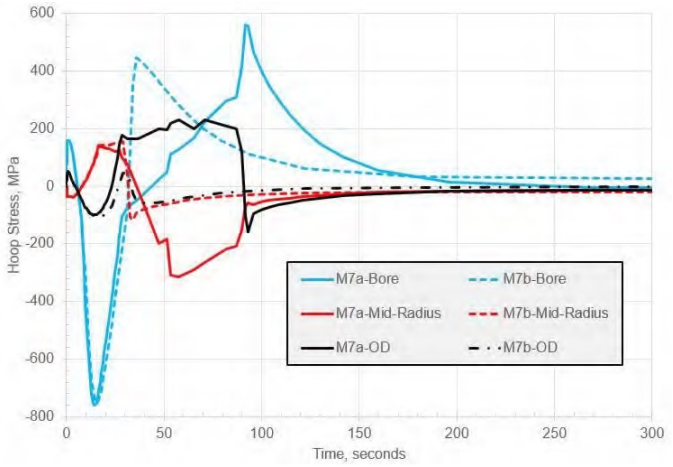

Figure 20. Hoop stress evolution at bore, mid-radius and outer diameter predicted for models 7a and 7b.

Discussion

Many figures have been presented that show effects of the magnitude of heat transfer, location of major quenching, and material kinetics on temperature change in the tube, phase transformation timing and stress state changes. An important question is how to make use of these results to select process conditions.

Another important question is whether it is better to quench the tube from the bore or from the outer diameter? Figure 21 compares the final hoop stress predictions for models 1, 5 and 7c that were intensively quenched on the bore, and model 2 that was intensively quenched on the outer diameter. If bore compression is desired, the models show that quenching the outer diameter produces a more extensive compressive zone than from bore quenching. Furthermore, the outer diameter is left under deep compression since the bore transformed to martensite much later than the OD. The dominant phase in all cases was martensite.

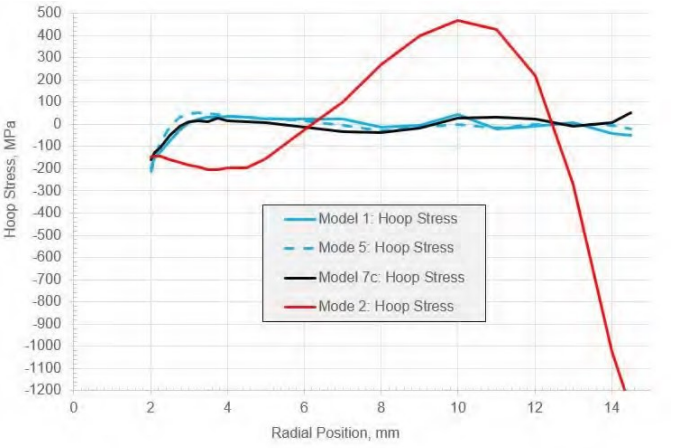

Figure 21. Predictions of residual hoop stress predictions for bore quenching and outer diameter quenching.

Furthermore, Figure 4 shows that the hoop stress on the bore rises to approximately +600 MPa as the outer layers of the tube form martensite and expand. This in-process stress may be high enough to cause a crack to form at the bore. KIT reported bore cracking during bore quenching[5]. Figure 7 shows that quenching from the outer diameter does not produce high in-process tension, lowering the possibility of quench cracking.

Conclusions

The many benefits of applying process modeling methods to investigate and improve manufacturing processes have been presented in reference 1-4. This paper has dealt with heat treatment, specifically looking at heat transfer during an intensive, novel quenching process for controlling the microstructure and residual stress in a small tube with a wall thickness of 12.5 mm made of 4140 steel.

The rate of martensite formation was shown to affect the temperature history of the tube due to the rate of latent heat generated. Rapid martensite formation, meaning that a small decrease in temperature led to a large increase in martensite content was predicted to cause an abrupt decrease in local cooling rate and even a thermal plateau while the latent heat could be dispersed by conduction. A lower rate of martensite formation allowed the latent heat to be conducted away with a reduced effect on local cooling rate.

Investigation of bore quenching vs. OD quenching in terms of stress state showed that a high rate of bore quenching produced higher stresses, especially at the bore and could lead to cracking. The final circumferential stress at the bore would have a magnitude of -100 to -200 MPa. However, for this tube size, quenching on the OD would reduce in-process tensile stress and result in a more compressive bore stress with levels of -1000 MPa. In both cases the bore and the main microstructural constituent would be martensite.

With enhanced bainite formation kinetics, bore quenching could be altered to reduce in-process stresses and increased residual hoop compression when martensite was formed in the bore and a mixture of matertensite and bainite was formed in the outer half of the tube cross section.

Computer simulation was used to obtain a more thorough understanding of the metallurgical events that occur during a rapid quenching process. These transient events are typically not intuitive because of the speed at which they occur and the nonlinearity of the metal's response to the rapidly changing temperature and microstructural state. With this type of process modeling tool, the benefits of process development and improvement can more quickly realized.

References

1. Maciej Pietrzyk, et al., Computational Materials Engineering: Achieving high accuracy and efficiency in metals processing simulations, Elsevier Inc., 2015.
2. Mark F. Horstemeyer, Integrated Computational Materials Engineering (ICME) for Metals: Using

Multiscale Modeling to Invigorate Engineering Design with Science, John Wiley & Sons, Inc., 2012.
3. Zhichao Li and B. Lynn Ferguson, “Heat Treatment and Fatigue of a Carburized and Quench Hardened Steel Part,” Chapter 5 of Integrated Computation Materials Engineering (ICME) for Metals: Concepts and Case Studies, Mark Horstemeyer, ed., John Wiley & Sons, Inc., pp 107-135, 2018.
4. Ronald A. Wallis, “Modeling of Quenching, Residual-Stress Formation, and Quench Cracking,” ASM Handbook Vol. 22B Metals Process Simulation, D.U. Furrer and S.L. Semiatin, eds., pp 547-585, 2010.
5. F. Muehl, S. Dietrich, and V. Schulze, “Internal Quenching: Ideal Heat Treatment for Difficult to Access Component Sections,” HTM J. Heat Treatment and Materials, v74 no3, pp 191-201, 2019.